

Pilot-tone based self-homodyne detection using optical nonlinear wave mixing

YINWEN CAO,^{1,*} MORTEZA ZIYADI,¹ AHMED ALMAIMAN,¹ AMIRHOSSEIN MOHAJERIN-ARIAEI,¹ PEICHENG LIAO,¹ CHANGJING BAO,¹ FATEMEH ALISHAHI,¹ AHMAD FALLAHPOUR,¹ BISHARA SHAMEE,¹ ASHER J. WILLNER,¹ YOUICHI AKASAKA,² TADASHI IKEUCHI,² STEVEN WILKINSON,³ CARSTEN LANGROCK,⁴ MARTIN M. FEJER,⁴ JOSEPH TOUCH,⁵ MOSHE TUR,⁶ AND ALAN E. WILLNER¹

¹ Department of Electrical Engineering, University of Southern California, Los Angeles, CA 90089, USA

² Fujitsu Laboratories of America, 2801 Telecom Parkway, Richardson, TX 75082, USA

³ Raytheon Company, El Segundo, CA 92195, USA

⁴ Edward L. Ginzton Laboratory, 348 Via Pueblo Mall, Stanford University, Stanford, CA 94305, USA

⁵ Information Sciences Institute, University of Southern California, Marina del Rey, CA 90292, USA

⁶ School of Electrical Engineering, Tel Aviv University, Ramat Aviv 69978, Israel

*Corresponding author: vinwenca@usc.edu

Received XX Month XXXX; revised XX Month, XXXX; accepted XX Month XXXX; posted XX Month XXXX (Doc. ID XXXXX); published XX Month XXXX

An all-optical pilot-tone based self-homodyne detection scheme using nonlinear wave mixing is experimentally demonstrated. Two scenarios are investigated using (i) multiple WDM channels with sufficient power of pilot tones, (ii) a single channel with a low-power pilot tone. The eye-diagram and bit-error-rate (BER) of the system are studied by tuning various parameters, such as pump power, relative phase, and pilot-to-signal ratio (PSR).

OCIS codes: (060.2920) Homodyning; (060.2360) Fiber optics links and subsystems; (060.4370) Nonlinear optics, fibers.

<http://dx.doi.org/10.1364/OL.99.099999>

Optical coherent detection is of importance in optical communication systems, especially for the recovery of sensitive phase-encoded data signals [1-3]. A coherent detection system notably requires phase and frequency locking between the incoming signal and the local oscillator (LO). Approaches to achieving a stable locking include the use of an optical phase-locked loop (OPLL) [4-6] or digital carrier recovery [7-10].

Self-homodyne detection (SHD) is another approach which can potentially simplify receiver signal processing [11] and relax the requirement for narrow linewidth lasers [12]. One common approach to realizing SHD relies on transmitting a pilot tone along with the data channel on another frequency or an orthogonal polarization. At the receiver, the pilot tone is extracted and processed in a different path that allows it to later beat with the data channel as an LO laser [11-14]. That approach requires

sufficient pilot-to-signal ratio (PSR) to ensure system performance [15,16] and it is typically accomplished by (i) transmitting a pilot tone with sufficient power, which reduces the effective data signal power that can be accommodated for transmission; or (ii) amplifying/regenerating a low-power co-transmitted pilot tone in a separate path at the receiver, which might require a phase-locked loop [13].

Recently, there has been another SHD method proposed using two stages of optical nonlinear wave mixing without sending a pilot tone [17]. By generating the delayed version of the incoming signal conjugate which is later mixed with the original signal, that approach can automatically lock a "local" pump to the signal without requiring a feedback loop controller. However, that approach (i) alters the original data encoding from quadrature-phase-shift-keying (QPSK) to differential QPSK by using an optical differentiator, and (ii) might be difficult to extend to a multi-channel wavelength-division-multiplexed (WDM) system.

In this paper, we demonstrate SHD that combines the use of the co-transmitted pilot tone and optical nonlinear wave mixing at the receiver. Our method is as follows: (i) at the transmitter, a pilot tone is placed at an adjacent frequency to a data channel; and (ii) at the receiver, phase-locked optical frequency comb lines are employed to convert the pilot tone to the center of the data channel spectrum [18,19]. This approach uses only a single nonlinear mixing stage to achieve automatic phase-locking for SHD without path separation or altering the data encoding. We demonstrate it with multiple WDM channels, each with its own pilot tone. In an experiment, two 20-Gbaud QPSK channels are recovered using a single periodically poled lithium niobate (PPLN)

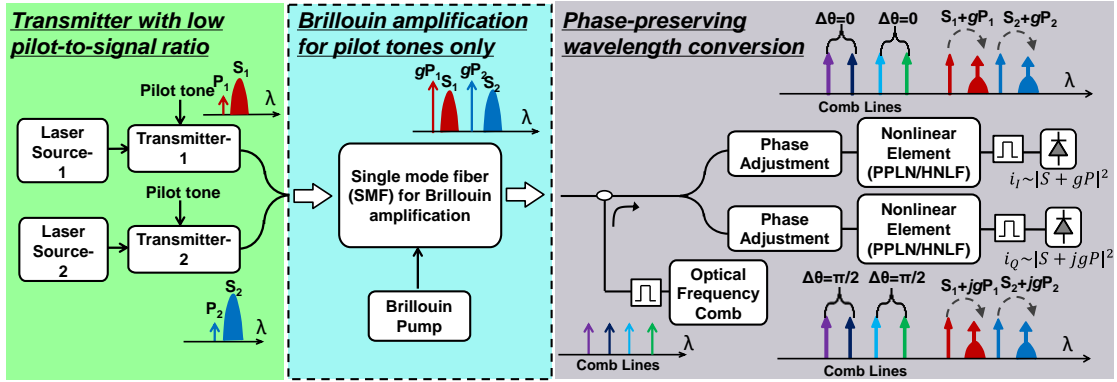


Fig. 1. Conceptual diagram of proposed self-homodyne detection (SHD) system. The scheme is composed of (i) Brillouin amplification to selectively amplify the pilot tones if pilot-to-signal ratio (PSR) is low, and (ii) phase-preserving wavelength conversion using optical frequency comb lines. The following two experiments demonstrate SHD for different scenarios: (i) WDM channels with sufficient PSR (without Brillouin amplification); (ii) a single channel with low PSR (with Brillouin amplification). PPLN: periodically poled lithium niobate; HNFL: highly nonlinear fiber.

waveguide. To address the power issue of the pilot tone, narrowband Brillouin amplification (BA) is added at the receiver for in-line selective amplification of the pilot tone. This achieves SHD for the channel with an ultra-low-power pilot tone. We experimentally demonstrate this scheme in a single channel of 10/20-Gbaud BPSK and 10-Gbaud QPSK signals. System performance can be maintained with a PSR as low as -30dB.

The concept of the proposed SHD system is shown in Fig. 1. At the transmitter, two data channels (S_1 and S_2) are sent with different pilot tones (P_1 and P_2). At the receiver, if the power of P_1 and P_2 are low (low PSR), a stage of BA is employed to selectively amplify the pilot tone by a gain coefficient of g without needing path separation [20,21]. In the next stage, the data channels (S_1, S_2) and the amplified pilot tones (gP_1, gP_2) are coupled with four phase-locked optical frequency comb lines to achieve phase-preserving wavelength conversion in a genetic nonlinear element, which could be a PPLN or a highly nonlinear fiber (HNFL) [22]. By choosing appropriate frequency difference (the frequency difference between S_i and P_i , $i=1, 2$) and relative phase ($\Delta\theta$) between the comb lines, the pilot tones are converted to the center of the data channel. Both I and Q components can be recovered using direct detection.

In the first experiment, the power of pilot tone is sufficiently high that BA can be bypassed. In Fig. 2, a mode-locked laser (MLL) with a 10GHz repetition rate is injected into a delay line interferometer (DLI) followed by a 450m HNFL to generate optical frequency comb lines with broad spectrum, as shown in Fig. 2(b1). A clock synchronizer is employed to maintain the repetition rate with a 10G clock reference. The transmitter and receiver share the comb lines, which are decorrelated by a 30km single mode fiber (SMF). In a spatial light modulator (SLM) filter at the transmitter, two comb lines are selected to be sent to an IQ modulator to generate 20-Gbaud QPSK signals. On the other port of the SLM filter, two other comb lines are selected as the corresponding pilot tones of the modulated signals. By sending these tones into injection locked lasers (ILL), they are amplified at the transmitter. The reason to use ILL is to make the scenario that the pilot tones have sufficient power at the transmitter side whereas the purpose of this experiment is to focus on the feasibility demonstration of SHD for multi-channel system. For channel decorrelation, each of the signals with its own pilot tone is sent through different fiber paths and later combined, with spectrum shown in Fig. 2(b2).

At the receiver, the signals with pilot tones are amplified and sent into a PPLN with a quasi-phase matching (QPM) wavelength of $\sim 1550.5\text{nm}$ along with the receiver's frequency comb lines. Inside the PPLN waveguide, the pilot tones are converted to the center of each of the data channels as shown in Fig. 2(b3). The desired signal is then filtered and sent to a PD for detection. Due to the path separation between the pilot tone and signal at the transmitter side, offline digital signal stabilization is employed to compensate the resultant phase variation based on a decision directed approach [23]. Because our available experimental setup has access to only a single PPLN (in contrast to the concept shown in Fig. 1), the two output paths (I and Q) of Fig. 1 have to be measured separately, each following proper adjustment of $\Delta\theta$ between the comb lines using SLM filter-2 as shown in Fig. 2(a). Figure 2(c) shows the eye diagrams for the two 20-Gbaud QPSK channels. The BER measurement is shown in Fig. 2(d). Compared to simultaneous multi-channel detection, separate channel detection could achieve a 1.8dB OSNR improvement at a BER of $1e-3$. The extra penalty might arise from the cross-talk in the PPLN, which is expected to increase if this approach is extended to larger number of channels. How to effectively suppress the cross-talk requires further research in the future.

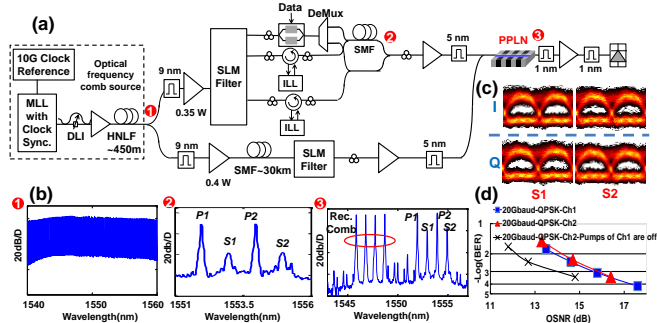


Fig. 2. (a) Experimental setup of SHD for WDM channels with high-power pilot tones without the middle part (Brillouin amplification) of Fig. 1; (b) corresponding spectra at each node; (c) eye diagrams of the two detected 20-Gbaud QPSK channels; (d) BER measurements. MLL: mode-locked laser; DLI: delay line interferometer; ILL: injection-locked laser; SLM: spatial light modulator.

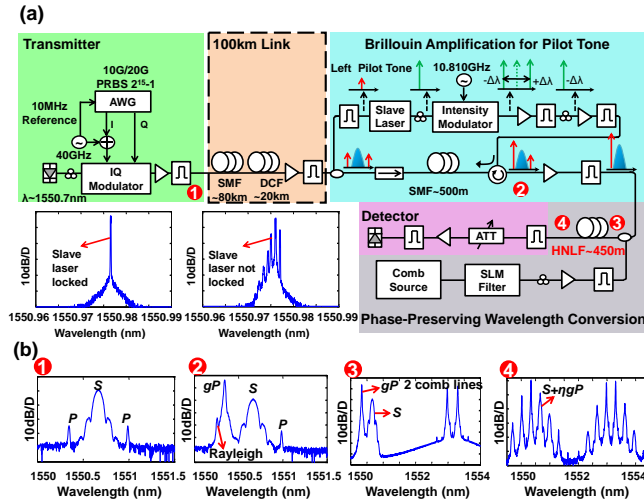


Fig. 3. (a) Experimental setup of SHD for a single channel with -30dB PSR and the spectra when the slave laser for Brillouin amplification is frequency locked or unlocked to the incoming pilot tone; (b) corresponding spectra measured at each node.

In the presence of a low-power co-transmitted pilot tone, the BA stage is included to boost power before the nonlinear wave mixing. The experimental setup of a single channel SHD with low PSR is shown in Fig. 3(a). At the transmitter, the data is generated using a high-speed arbitrary waveform generator (AWG), and the I component is added with a low-power sinusoidal pilot tone generated by a 40GHz clock synthesizer. The clock in the AWG is frequency locked with the pilot tone clock by a 10MHz reference. Then, the data signal modulates a laser at the wavelength of 1550.7nm in an IQ modulator. The spectrum of the signal with pilot tone is shown in Fig. 3 (b1), where the launch power is 3dBm and the PSR is -30dB. The signal with the pilot tone is sent to either (i) the proposed SHD structure directly for B2B evaluation, or (ii) a 100-km link comprising an 80km SMF and a 20km dispersion compensated fiber (DCF) with a total loss of 30.7dB.

At the receiver, the incoming signal with pilot tone is sent to two paths. In the upper path, the left pilot tone is selected by a narrowband optical filter and sent to a slave laser that is frequency-locked to the input pilot tone. Compared to [24,25], which require a phase locking of ILL, the slave laser is used as a BA pump so that phase locking is not required. The temperature and current of the slave laser need to be tuned for frequency locking. The output is then modulated by a 10.810GHz sinusoidal tone in an intensity modulator biased at the null point. The generated lower sideband (higher frequency) continuous waveform (CW) is selected and amplified to act as the BA pump, as shown in Fig. 3(a). Afterwards, the BA pump propagates in the opposite direction to the incoming signal in a 500m SMF, in which only the pilot tone is amplified by ~40dB with the narrowband Brillouin interaction, as shown in Fig. 3(b2). The signal with pilot tone is then amplified in an EDFA and sent into a narrowband optical filter, in which the Rayleigh back-scattering component is suppressed. In the next stage, the same comb source in Fig. 2(b1) are sent to a SLM filter and two comb lines with a 40GHz frequency difference are selected with appropriate phase adjustment. Then, the two comb lines are amplified before sending them to a 450m HNLF. The complete spectra before and after the HNLF are shown in Fig. 3(b3) and Fig. 3(b4), in which the amplified pilot tone is converted to the

middle of the data spectrum. In the experiment, the frequency spacing between the signal and pilot tone is manually tuned to align with the frequency spacing between the two comb lines. For the practical implementation in which the transmitter and receiver are at different locations, a simple digital frequency offset estimation and compensation [26] would be required. Finally, the data channel is filtered and sent to a PD for real-time eye-diagram capture and BER measurement. For the BER measurement of an IQ modulation format such as QPSK, the reported BER is the average of the separate measurements for I and Q components.

The narrowband characteristic of the BA is illustrated in Fig. 4(a). The frequency offset denotes the frequency drift away from the optimal Brillouin frequency shift in the SMF of the experiment, measured as 10.810GHz. The BA gain drops to zero when the frequency offset is ~45MHz. Figure 4(b) shows the relationship between Brillouin pump power and BA gain, where a 150mw pump produces a ~40dB gain on the pilot tone with -34dBm power at the input of the 500m SMF.

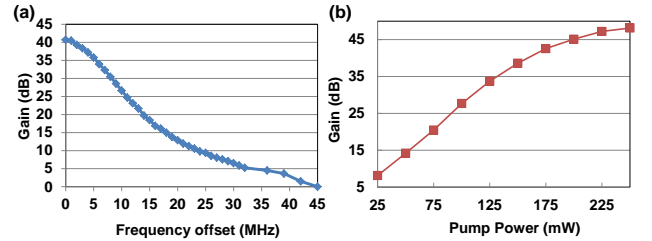


Fig. 4. (a) Bandwidth of Brillouin amplification; (b) gain variation of Brillouin amplification for the pilot tone by changing the pump power.

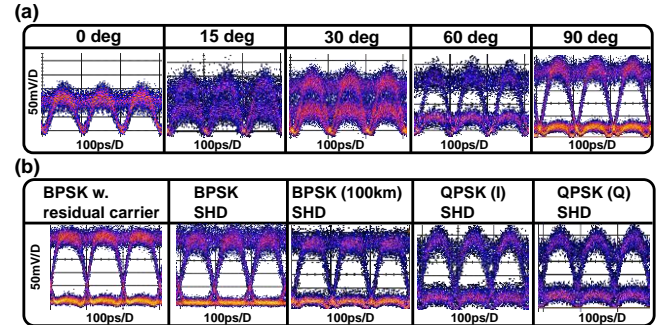


Fig. 5. (a) The detected eye diagram of BPSK varies with $\Delta\theta$ between two comb lines; (b) detected eye diagrams for a 10-Gbaud system with different modulation formats.

System performance is evaluated using 10-Gbaud BPSK and QPSK channels, each with -30 dB PSR. Figure 5(a) shows that the eye-diagram opens and closes with $\Delta\theta$ between the two comb lines in Fig. 3(b3). Figure 5(b) presents the eye-diagrams for different modulation formats. As a baseline for comparison, a 10-Gbaud BPSK signal with a residual carrier in the center is sent directly to the PD. Compared to the baseline system, the proposed SHD has a relatively higher noise level which is attributed to the extra spontaneous Brillouin noise during pilot tone boosting by BA. After a 100km transmission, the signal quality degrades a little further, which might be caused by the residual chromatic dispersion of the link. By adjusting $\Delta\theta$, the I and Q components of the QPSK signal are obtained, as shown in Fig. 5(b).

The real-time BER of a 10-Gbaud channel is measured, as shown in Fig. 6(a). The received power is measured after the attenuator in the detector part of Fig. 3(a). Compared to the ideal case, the B2B BPSK has a similar BER curve. After the 100km link, a power penalty of ~ 0.5 dB is observed at the FEC limit (BER = 3.8×10^{-3}). For a QPSK signal, a power penalty of 4dB is observed at the FEC limit. A BER comparison with a 20-Gbaud BPSK signal is shown in Fig. 6(b) to demonstrate the tunability of the scheme. Compared to the 20-Gbaud BPSK baseline, a power penalty of ~ 0.5 dB is observed at the FEC limit. Received power could also be measured before the BA stage (after the 100km link). However, since the signal would experience degradation after two stages of SHD, the same received power would yield a higher BER. The result would be that, except for the baseline curve, the curves would have shifted to the right.

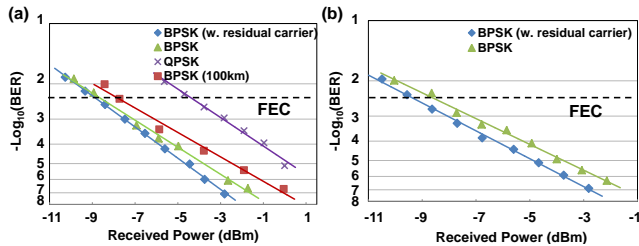


Fig. 6. BER for (a) 10-Gbaud BPSK/QPSK, and (b) 20-Gbaud BPSK.

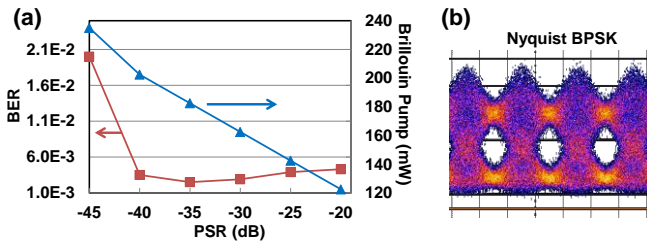


Fig. 7. (a) BER measurements for different levels of PSR and the corresponding Brillouin pump power with -8.4 dBm received power; (b) eye diagram of 10-Gbaud Nyquist BPSK signal.

B2B system performance is also investigated for different PSRs, while the received power is kept at -8.4 dBm. Figure 7(a) shows that as PSR decreases, the power of the Brillouin pump needs to be increased to maintain the same output power of the amplified pilot tone. Therefore, output PSR remains the same, which produces a relatively constant BER. The proposed scheme can even work with a PSR as low as -40 dB. When the PSR further decreases to -45 dB, the slave laser fails to lock to the faint input pilot tone, and the BER dramatically increases. The proposed scheme is also verified with Nyquist pulse shaping of 0.01 rolling off factor, as shown in Fig. 7(b). This scheme could potentially be extended to WDM system with low PSR, which requires multiple BA pumps to be generated accordingly [27]. It is noted that the pilot tone is separated from the data channel by a 40GHz gap. For WDM applications, this placement may affect the spectrum efficiency. Moving the pilot tone closer to the data spectrum would alleviate this problem. However, the resultant interference from the data spectrum could degrade the quality of the pilot tone. Therefore, optimizing the location of the pilot tone requires further investigation.

In this paper, BPSK/QPSK are employed only to demonstrate the concept of the proposed SHD system, which is based on high-

speed optical nonlinear wave mixing. Compared to conventional differential detection [28] and digital phase tracking [29] for BPSK/QPSK, the SHD complexity might be higher. However, SHD is expected to relax encoder and decoder design restrictions in differential detection schemes for MPSK signals [30]. Also, SHD could be important for high order QAM with increased data rate, in which high-speed digital processing for phase tracking might be a challenge [12]. In addition, the ability of this approach to support multiple-channel SHD realization could be of interest in the future.

Funding. Center for Integrated Access Networks (CIAN); Fujitsu Laboratories of America (FLA); National Science Foundation (NSF)

References

- P. J. Winzer, *IEEE Comm. Mag.* **48**, 26 (2010).
- E. Ip, A. Lau, D. Barros, and J. Kahn, *Opt. Exp.* **16**, 753 (2008).
- M. G. Taylor, *Photon. Technol. Lett.* **16**, 674 (2004).
- L. Kazovsky, *J. Lightw. Technol.* **2**, 182 (1986).
- S. Ristic, A. Bhardwaj, M. J. Rodwell, L. A. Coldren and L. A. Johansson, *J. Lightw. Technol.* **28**, 526 (2010).
- M. Lu, H. Park, E. Bloch, A. Sivanathan, A. Bhardwaj, Z. Griffith, L. A. Johansson, M. J. Rodwell, and L. A. Coldren, *Opt. Exp.* **20**, 9736 (2012).
- X. Zhou, *Photon. Technol. Lett.* **22**, 1051 (2010).
- A. Viterbi, *IEEE Trans. Info. Theory* **29**, 543 (1983).
- I. Fatadin, D. Ives and S. J. Savory, *Photon. Technol. Lett.* **22**, 631 (2010).
- T. Pfau, S. Hoffmann, and R. Noé, *J. Lightw. Technol.* **27**, 989 (2009).
- Z. Vujčić, R. S. Luis, J. Mendinueta, A. Shahpari, N. B. Pavlović, B. J. Puttnam, Y. Kamio, M. Nakamura, N. Wada, and A. Teixeira, *Photon. Technol. Lett.* **27**, 2226 (2015).
- M. Nakamura, Y. Kamio, and T. Miyazaki, *Opt. Exp.* **16**, 10611 (2008).
- A. Chiuchiarrelli, M. Fice, E. Ciaramella, and A. Seeds, *Opt. Exp.* **19**, 1707 (2011).
- K. Kasai, S. Beppu, Y. Wang, and M. Nakazawa, *Proc. OFC, W1E.4* (2015).
- T. Kobayashi, A. Sano, A. Matsuura, Y. Miyamoto and K. Ishihara, *J. Lightw. Technol.* **30**, 3805 (2012).
- T. Huynh, L. Nguyen, V. Vujicic and L. Barry, *J. Opt. Comm. Netw.* **6**, 152 (2014).
- M. Chitgarha, A. Mohajerin-Ariaei, Y. Cao, M. Ziyadi, S. Khaleghi, A. Almainan, J. Touch, C. Langrock, M. Fejer, and A. Willner, *J. Lightw. Technol.* **33**, 1344 (2015).
- M. Ziyadi, A. Mohajerin Ariaei, M. Chitgarha, Y. Cao, A. Almainan, Y. Akasaka, J. Yang, G. Xie, P. Liao, M. Sekiya, J. Touch, M. Tur, C. Langrock, M. Fejer and A. Willner, *Proc. CLEO, STh10.6* (2015).
- Y. Cao, A. Almainan, M. Ziyadi, P. Liao, A. Mohajerin Ariaei, F. Alishah, C. Bao, A. Fallahpour, B. Shamee, A. Willner, A. Youichi, T. Ikeuchi, S. Wilkinson, J. Touch, M. Tur, and A. Willner, *Proc. OFC, M2A.6* (2016).
- N. A. Olsson and J. van der Ziel, *Appl. Phys. Lett.* **48**, 1329 (1986).
- L. Banchi, M. Presi, R. Proietti, and E. Ciaramella, *Opt. Exp.* **18**, 12702 (2010).
- G. Lu, T. Bo, T. Sakamoto, N. Yamamoto, and C. Chan, *Opt. Exp.* **24**, 22573 (2016).
- X. Zhou and J. Yu, *J. Lightw. Technol.*, **27**, 3641 (2009).
- A. Albores-Mejia, T. Kaneko, E. Banno, K. Uesaka, H. Shoji, and H. Kuwatsuka, *Proc. ECOC, Tu.3.1.4* (2014).
- K. Kasai, Y. Wang, S. Beppu, M. Yoshida, and M. Nakazawa, *Opt. Exp.* **23**, 29174 (2015).
- A. Leven, N. Kaneda, U. V. Kco, and Y. K. Chen, *Photon. Technol. Lett.* **19**, 366 (2007).
- A. Lorences-Riesgo, M. Mazur, T. Eriksson, P. Andrekson, and M. Karlsson, *Opt. Exp.* **24**, 29714 (2016).
- R. Griffin and A. Carter, *Proc. OFC, 2002*, paper WX6.
- R. Noé, *J. Lightw. Technol.* **23**, 802 (2005).
- T. Miyazaki, *Photon. Technol. Lett.* **18**, 388 (2006).

References (Long Format)

1. P. J. Winzer, "Beyond 100G Ethernet," in *IEEE Communications Magazine*, vol. 48, no. 7, pp. 26-30, 2010.
2. Ezra Ip, Alan Pak Tao Lau, Daniel J. F. Barros, and Joseph M. Kahn, "Coherent detection in optical fiber systems," in *Optics Express*, vol. 16, no. 2, pp. 753-791, 2008.
3. M. G. Taylor, "Coherent detection method using DSP for demodulation of signal and subsequent equalization of propagation impairments," in *Photonics Technology Letters*, vol. 16, no. 2, pp. 674-676, 2004.
4. L. Kazovsky, "Balanced phase-locked loops for optical homodyne receivers: Performance analysis, design considerations, and laser linewidth requirements," in *Journal of Lightwave Technology*, vol. 4, no. 2, pp. 182-195, 1986.
5. S. Ristic, A. Bhardwaj, M. J. Rodwell, L. A. Coldren and L. A. Johansson, "An Optical Phase-Locked Loop Photonic Integrated Circuit," in *Journal of Lightwave Technology*, vol. 28, no. 4, pp. 526-538, 2010.
6. M. Lu, H. Park, E. Bloch, A. Sivanathan, A. Bhardwaj, Z. Griffith, L. Johansson, M. Rodwell, and L. Coldren, "Highly integrated optical heterodyne phase-locked loop with phase/frequency detection," in *Optics Express*, vol. 20, no. 9, pp. 9736-9741, 2012.
7. X. Zhou, "An improved feed-forward carrier recovery algorithm for coherent receivers with M-QAM modulation format," in *Photonics Technology Letters, IEEE*, vol. 22, no. 14, pp. 1051-1053, 2010.
8. A. Viterbi, "Nonlinear estimation of PSK-modulated carrier phase with application to burst digital transmission," in *Information Theory, IEEE Transactions on*, vol. 29, no. 4, pp. 543-551, 1983.
9. I. Fatadin, D. Ives and S. J. Savory, "Laser Linewidth Tolerance for 16-QAM Coherent Optical Systems Using QPSK Partitioning," in *Photonics Technology Letters*, vol. 22, no. 9, pp. 631-633, 2010.
10. T. Pfau, S. Hoffmann, and R. Noé, "Hardware-Efficient Coherent Digital Receiver Concept with Feedforward Carrier Recovery for M-QAM Constellations," in *Journal of Lightwave Technology*, vol. 27, no. 8, pp. 989-999, 2009.
11. Z. Vujčić, R. S. Luís, J. Mendinueta, A. Shahpari, N. B. Pavlović, B. J. Puttnam, Y. Kamio, M. Nakamura, N. Wada, and A. Teixeira, "Self-Homodyne Detection-Based Fully Coherent Reflective PON Using RSOA and Simplified DSP," in *Photonics Technology Letters*, vol. 27, no. 21, pp. 2226-2229, 2015.
12. M. Nakamura, Y. Kamio, and T. Miyazaki, "Linewidth-tolerant 10-Gbit/s 16-QAM transmission using a pilot-carrier based phase-noise cancelling technique," in *Optics Express*, vol. 16, no. 14, pp. 10611-10616, 2008.
13. A. Chiuchiarrelli, M. J. Fice, E. Ciaramella, and A. J. Seeds, "Effective homodyne optical phase locking to PSK signal by means of 8b10b line coding," in *Optics Express*, vol. 19, no. 3, pp. 1707-1712, 2011.
14. K. Kasai, S. Beppu, Y. Wang, and M. Nakazawa, "256 QAM (Polarization-multiplexed, 5 Gsymbol/s) Coherent Transmission with an Injection-locked Homodyne Detection Technique," in *Optical Fiber Communication Conference, OSA Technical Digest (online) (Optical Society of America, 2015)*, paper W1E.4.
15. T. Kobayashi, A. Sano, A. Matsuura, Y. Miyamoto and K. Ishihara, "Nonlinear Tolerant Spectrally-Efficient Transmission Using PDM 64-QAM Single Carrier FDM With Digital Pilot-Tone," in *Journal of Lightwave Technology*, vol. 30, no. 24, pp. 3805-3815, 2012.
16. T. N. Huynh, L. Nguyen, V. Vujicic and L. P. Barry, "Pilot-tone-aided transmission of high-order QAM for optical packet switched networks," in *IEEE/OSA Journal of Optical Communications and Networking*, vol. 6, no. 2, pp. 152-158, 2014.
17. M. R. Chitgarha, A. Mohajerin-Ariaei, Y. Cao, M. Ziyadi, S. Khaleghi, A. Almainan, J. Touch, C. Langrock, M. Fejer, and A. Willner, "Tunable Homodyne Detection of an Incoming QPSK Data Signal Using Two Fixed Pump Lasers," in *Journal of Lightwave Technology*, vol. 33, no. 7, pp. 1344-1350, 2015.
18. M. Ziyadi, A. Mohajerin Ariaei, M. R. Chitgarha, Y. Cao, A. Almainan, Y. Akasaka, J. Y. Yang, G. Xie, P. Liao, M. Sekiya, J. Touch, M. Tur, C. Langrock, M. Fejer and A. E. Willner, "Demonstration of tunable and automatic frequency/phase locking for multiple-wavelength QPSK and 16-QAM homodyne receivers using a single nonlinear element," in 2015 Conference on Lasers and Electro-Optics (CLEO), San Jose, CA, 2015, pp. 1-2.
19. Y. Cao, A. Almainan, M. Ziyadi, P. Liao, A. Mohajerin Ariaei, F. Alishah, C. Bao, A. Fallahpour, B. Shamee, A. Willner, A. Youichi, T. Ikeuchi, S. Wilkinson, J. Touch, M. Tur, and A. Willner, "Demonstration of Automatically Phase-Locked Self-Homodyne Detection with a Low-Power Pilot Tone based on Brillouin Amplification and Optical Frequency Combs," in *Optical Fiber Communication Conference, OSA Technical Digest (online) (Optical Society of America, 2016)*, paper M2A.6.
20. N. A. Olsson and J. van der Ziel, "Cancellation of fiber loss by semiconductor laser pumped Brillouin amplification at 1.5 μm ," in *Applied Physics Letters*, vol. 48, pp. 1329-1330, 1986.
21. L. Banchi, M. Presi, R. Proietti, and E. Ciaramella, "System feasibility of using stimulated Brillouin scattering in self coherent detection schemes," in *Optics Express*, vol. 18, no. 12, pp. 12702-12707, 2010.
22. G. Lu, T. Bo, T. Sakamoto, N. Yamamoto, and C. Chan, "Flexible and scalable wavelength multicast of coherent optical OFDM with tolerance against pump phase-noise using reconfigurable coherent multi-carrier pumping," in *Optics Express*, vol. 24, no. 20, pp. 22573-22580, 2016.
23. X. Zhou and J. Yu, "Multi-Level, Multi-Dimensional Coding for High-Speed and High-Spectral-Efficiency Optical Transmission," in *Journal of Lightwave Technology*, vol. 27, no. 16, pp. 3641-3653, 2009.
24. A. Albores-Mejia, T. Kaneko, E. Banno, K. Uesaka, H. Shoji, and H. Kuwatsuka, "Hardware efficient QAM16 all-optical carrier recovery using a single optically-stabilized injection-locked semiconductor laser," in *Proceedings of the Euro. Conf. on Optical Communication (ECOC), Cannes, 2014, Tu.3.1.4*.
25. K. Kasai, Y. Wang, S. Beppu, M. Yoshida, and M. Nakazawa, "80 Gbit/s, 256 QAM coherent transmission over 150 km with an injection-locked homodyne receiver," in *Optics Express*, vol. 23, no. 22, pp. 29174-29183, 2015.
26. A. Leven, N. Kaneda, U. V. Kco, and Y. K. Chen, "Frequency estimation in intradyne reception," in *Photonics Technology Letters*, vol. 19, no. 6, pp. 366-368, 2007.
27. A. Lorences-Riesgo, M. Mazur, T. Eriksson, P. Andrekson, and M. Karlsson, "Self-homodyne 24x32-QAM superchannel receiver enabled by all-optical comb regeneration using brillouin amplification," in *Optics Express*, vol. 24, no. 26, pp. 29714-29723, 2016.
28. R. Griffin and A. Carter, "Optical differential quadrature phase-shift key (oDQPSK) for high capacity optical transmission," in *Optical Fiber Communication Conference, OSA Technical Digest (online) (Optical Society of America, 2002)*, paper WX6.
29. R. Noé, "Phase noise tolerant synchronous QPSK/BPSK baseband type intradyne receiver concept with feedforward carrier recovery," in *Journal of Lightwave Technology*, vol. 23, no. 2, pp. 802-808, 2005.
30. T. Miyazaki, "Linewidth-tolerant QPSK homodyne transmission using a polarization-multiplexed pilot carrier," in *Photonics Technology Letters*, vol. 18, no. 2, pp. 388-390, 2006.